JOC The Journal of Organic Chemistry

Article

Helical Chirality Induces a Substrate-Selectivity Switch in Carbohydrates Recognitions

Augustin Long, Olivier Perraud, Muriel Albalat, Vincent Robert, Jean-Pierre Dutasta, and Alexandre Martinez

J. Org. Chem., **Just Accepted Manuscript** • DOI: 10.1021/acs.joc.8b00276 • Publication Date (Web): 08 May 2018

ACS Publications

is published by the American Chemical Society. 1155 Sixteenth Street N.W., Washington, DC 20036

Helical Chirality Induces a Substrate-Selectivity Switch in Carbohydrates Recognitions

Augustin Long[†], Olivier Perraud[‡], Muriel Albalat[†], Vincent Robert[§], Jean-Pierre Dutasta[‡], Alexandre Martinez*[,†]

[†] Aix Marseille Univ, CNRS, Centrale Marseille, iSm2, Marseille, France

E-mail: alexandre.martinez@centrale-marseille.fr

[‡] Laboratoire de Chimie

École Normale Supérieure de Lyon, CNRS, UCBL

46, Allée d'Italie, F-69364 Lyon, France

[§] Laboratoire de Chimie Quantique Institut de Chimie, UMR CNRS 7177,

Université de Strasbourg, 4, rue Blaise Pascal,

F-67070 Strasbourg, France.

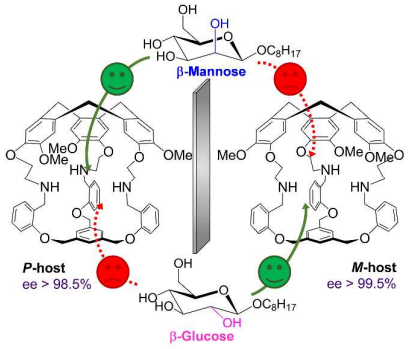

Abstract. A new chiral hemicryptophane cage combining electron rich CTV unit and polar amine functions has been synthesized. The resolution of the racemic mixture has been performed by chiral HPLC, and the assignment of the absolute configuration of the two enantiomers has been achieved using ECD spectroscopy. In contrast with other hemicryptophane receptors, the two enantiomeric hosts display both remarkable enantioselectivities in the recognition of carbohydrates and good binding constants. Moreover, by switching the chirality of the CTV unit from *M* to *P*, a strong preference shift from glucose to mannose derivatives is observed.

Introduction

The recognition of carbohydrates plays a crucial role in many biological processes, like tumor metastases,[1] protein folding,[2] infection by pathogens[3] or cell-cell recognition.[4] Their chirality can account for their versatile use in living systems: sugars can be considered as the most information-rich biological molecules as they present numerous stereogenic centers. Thus, biological systems have developed selective receptors in order to exploit this structural variability. The selective recognition of carbohydrates by synthetic receptors through non-covalent interactions arouse a considerable interest as it could allow for a better understanding of these biological processes and lead to the establishment of new diagnostics or therapies in medicine.[5-7] However, carbohydrates stereoisomers are very difficult to discriminate by synthetic hosts as they present complex three-dimensional structures, which often only differ by the configuration of a single stereogenic centre. Cage receptors, when compared to their "open-shell" counterparts,[8] appear as particularly appealing because they can maximize the interactions with sugar guests in the heart of their cavity leading to a better selectivity.[9] Among the cage compounds, hemicryptophanes have been recently described as a new class of receptors capable of complexing carbohydrates.[10] These hosts, built from a cyclotriveratrylene (CTV) linked to another C_3 symmetrical moiety, display low to good binding constants and selectivities toward sugar guests. However, this class of host suffers from a major drawback in carbohydrates recognition: either hemicryptophanes display good binding constants but a low selectivity, or a high selectivity is reached but associated with a modest affinity. For instance, host **1** exhibits good binding constants toward mannose up to 10^3 M^{-1}, but negligible enantioselectivity is observed (binding constants are 1410 and 1544 M^{-1} for the recognition of Oct-α-Man with *M*-*SSS*-**1** and *P*-*RRR*-**1**, respectively, Figure 1),[11] whereas host **2** shows an exclusive enantioselectivity toward Oct-α-Glc derivative, but a much modest association constant of around 155 M^{-1} is measured with the *M*-*SSS* enantiomer.[12] Thus, there is a challenge to design new hemicryptophane cages capable of combining both good affinity and selectivity toward carbohydrates. Here we report on the synthesis of the enantiopure hemicryptophanes (-)-**3** and (+)-**3**. Resolution of the racemic mixture has been achieved by chiral HPLC and assignment of their absolute configuration by electronic circular dichroism (ECD). Their recognition properties towards mannose, glucose and galactose derivatives reveal that both good binding constants (up to 10^3 M^{-1}) and enantioselectivity (> 99.5/0.5), can be achieved with host **3**. Interestingly, the change in the

helical chirality of the CTV unit induces a substrate-selectivity switch: the *M*-(-)-**3** enantiomer shows a better binding constant toward β-glucose derivative whereas the *P*-(+)-**3** enantiomer exhibits a remarkable selectivity for mannose.

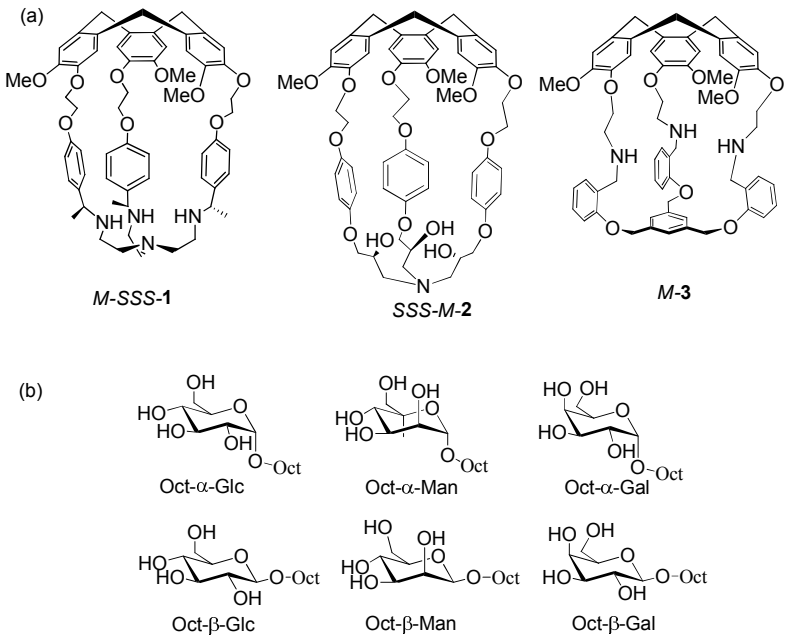

Figure 1. (a) Structures of hemicryptohane hosts **1**-**3**. (b) Structures of the carbohydrate guests.

Results and discussion

Synthesis

Scheme 1 shows the synthetic pathway followed to synthesize the hemicryptophane *rac*-**3**. Cyclotriveratrylene derivative **4** was obtained according to the previously reported two steps procedure: vanillyl alcohol first reacts with 1,2-dibromoethane and the subsequent cyclization achieved with scandium triflate in CH_3CN, provides the CTV *rac*-**4** in 18 % overall yield.[13] The reaction between sodium azide and *rac*-**4** affords *rac*-**5** in 90% yield. The reduction of the azido groups of *rac*-**5** is performed with PPh_3 in a mixture of THF and water at room temperature to give *rac*-**6** in 91% yield. The C_3 symmetrical derivative **7** is obtained by reaction between 1,3,5-tribromomethyl-benzene and 2-hydroxybenzaldehyde with NaOH in EtOH. Reductive amination between **7** and *rac*-**6** is then achieved in a $CHCl_3$/MeOH mixture providing *rac*-**3** in 42% yield. Thus,

hemicryptophane *rac*-**3** was obtained with a six-step convergent synthesis, starting from the commercially available vanillyl alcohol with an overall yield of 6%.

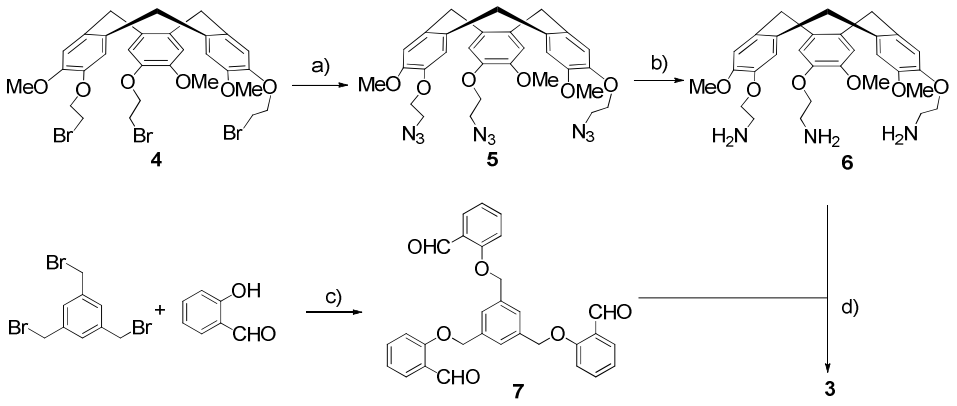

Scheme 1. Synthesis of *rac*-**3**; a) NaN_3, DMF, 60°C, 16h, 90%; b) PPh_3, THF/H_2O (30/1), r.t., 16h, 91%; c) NaOH, EtOH, reflux, 20h, 78%; d) (i) $CHCl_3$/MeOH (1/1), r.t., 18h; (ii) $NaBH_4$, 0°C to r.t.; 3h, 42%.

The resolution of the racemic mixture of hemicryptophane **3** is performed using chiral HPLC. The enantiomers are separated on analytical Chiralpak ID (250 x 4,6 mm) column with resolution higher than two (Table S1). The use of a semi-preparative Chiralpak ID (250 x 10 mm) column with EtOH+Et_3N/CH_2Cl_2 (50/50) as eluent, affords the (-)-enantiomer and (+)-enantiomer with ee > 99.5% and 98.5% respectively (Figures S16 and S17).

The hemicryptophanes (-)-**3** and (+)-**3** are on average of C_3 symmetry in solution as indicated by their ^{1}H NMR spectra in $CDCl_3$. That of (+)-**3** is shown in Figure 2 and displays the expected signals for the CTV moiety: the characteristic AB system for the $ArCH_2$ bridges at 3.53 and 4.73 ppm, two singlets for the aromatic protons at 6.90 and 6.75 ppm and one singlet for the OMe group. The aromatic protons of the benzene ring in the lower part of the host appear as a singlet at 6.82 ppm and the connected diastereotopic methylene bridges appear as two multiplets between 4.20 and 4.35 ppm. The signals of the aromatic protons of the linkers give two doublets and two triplets between 6.5 and 7.2 ppm, whereas the diastereotopic aliphatic protons exhibit expected broad multiplets.

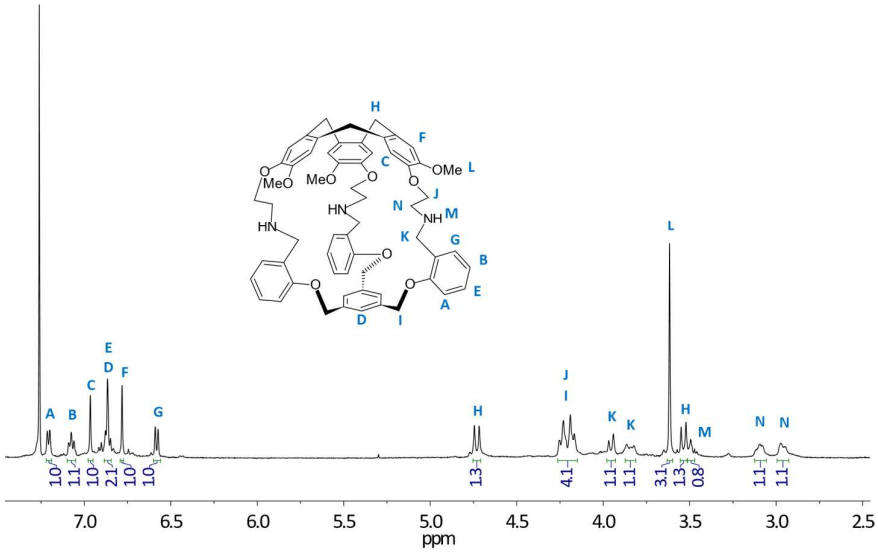

Figure 2. ^{1}H NMR spectra (400 MHz, $CDCl_3$) of (+)-**3.**

Assignment of the absolute configuration

The ECD spectra of hosts *P*-**3** and *M*-**3** were recorded in CH_2Cl_2 at 298 K (Figure 3). Each spectrum exhibits the expected behavior for hemicryptophanes and CTV based host compounds, namely two exciton patterns roughly centered on the isotropic absorption of the $^{1}L_B$ (290 nm) and $^{1}L_A$ (240 nm) transitions. As the signs of the ECD spectra in the $^{1}L_A$ transition area are poorly sensitive to the nature of the substituents, the assignment of the absolute configuration of CTV's is usually performed by comparison to the calculated ECD spectra of a reference CTV, previously obtained by Collet and co-workers.[14] Based on these previous works, the first (respectively second) eluted compound (+)-**3** (respectively (-)-**3**) corresponds to the *P* configuration (respectively *M* configuration).

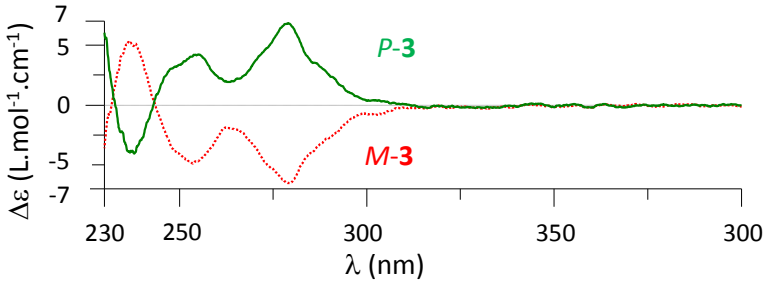

Figure 3. Experimental ECD spectra of the enantiomers of **3**: the first eluted enantiomer is represented with a green solid line (0.404 mmol.L^{-1} in CH_2Cl_2) and the second one by a red dotted line (0.442 mmol.L^{-1} in CH_2Cl_2).

Recognition properties

The inner cavity of hemicryptophane **3** presents both apolar (north and south parts) and polar domains (NH groups in the linkers) and thus, should provide appropriate matches for sugars complexation through C-H···π interactions and hydrogen bonding respectively. Additions of a solution of Oct-β-Glc in $CDCl_3$ to a solution of the enantiomer (-)-**3** in the same solvent induce changes in the chemical shift of the ^1H signals of the cage, evidencing interactions between the sugar guest and the hemicryptophane host. The formation of a host-guest complex is also supported by mass spectrometry: a peak with an exact mass corresponding to the 1:1 host:guest ratio was detected in a mixture of (-)-**3** and Oct-β-Glc (Figure S20). Insights into the positioning of the carbohydrate inside the cavity of the hemicryptophane (-)-**3** can be retrieved from the NOESY experiments performed on an equimolar solution of Oct-β-Glc and (-)-**3**.[15,16] Although several signals overlap, precluding the assignment of the whole intermolecular contacts, the following intermolecular host/guest NOEs contacts are unambiguously evidenced in the NOESY map: OMe/H_1 and CTV-H_{ar}/H_3 (Figure 4). These data strongly support the formation of an inclusion complex of Oct-β-Glc inside the cavity of (-)-**3**. It can be underlined that with other hemicryptophane derivatives, previously reported as receptors for carbohydrates, NOEs were never observed, suggesting that this Oct-β-Glc@(-)-**3** complex is kinetically more stable in solution, than the previously reported hemicryptophane complexes, although the host-guest exchange remains fast on the NMR time scale.[9-12,17] Based on these intermolecular NOEs contacts, DFT calculations were then performed in order to provide a three dimensional structure of the complex. The resulting minimized structure is shown in Figure 5 and is in agreement with the NOE experimental data (H_1···OMe and H_3···CTV-H_{ar} distances of 2.5 and 3.9 Å respectively). Furthermore, the optimized geometry of the complex reveals that Oct-β-Glc is partially encaged in the hemicryptophane structure with the sugar unit trapped inside the cavity and the alkyl chain left outside. Hydrogen bonding between the alcohol functions of the guest and the nitrogen of the host **3** are observed (for instance, NH···O_4 and NH···O_1 distances of 2.68 and 2.65 Å are measured respectively). CH···π interactions are also evidenced in the DFT structure with H_1··· CTV-C and H_4···C-Ar distances of 2.57 and 2.75 Å respectively.

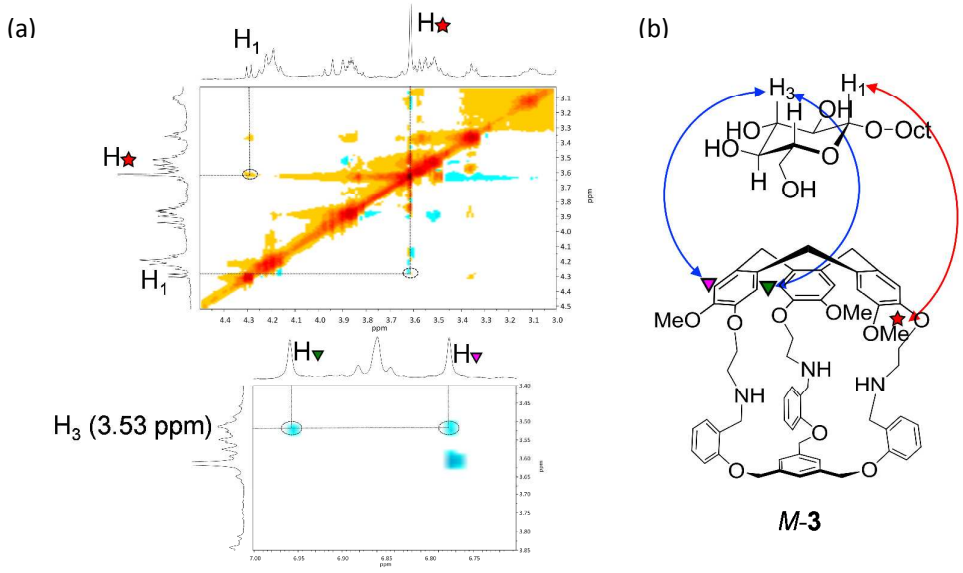

Figure 4. (a) 400 MHz NOESY spectrum of a 1:1 mixture of Oct-β-Glc and (-)-**3** in $CDCl_3$ at 298 K, acquired with a 500 ms mixing time. (b) Schematic representation of NOE contacts.

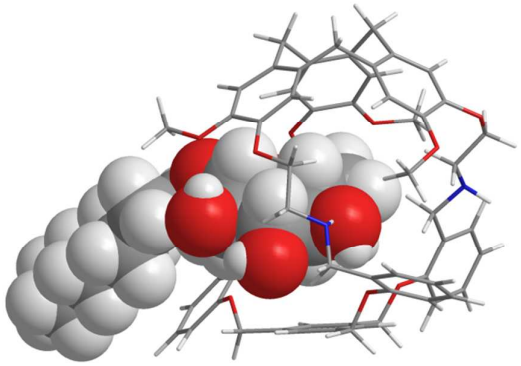

Figure 5. DFT optimized structure showing the encapsulation of Oct-β-Glc guest within hemicryptophane (-)-**3**.

We then investigated the ability of the enantiomeric hosts to discriminate stereoisomeric carbohydrates. ^{1}H NMR titration experiments between the two enantiomers of receptor **3** and six carbohydrates (α- and β-mannose, α- and β-glucose and α- and β-galactose, Figure 1) were thus performed in $CDCl_3$ at 298 K. In all cases only one set of signals was observed for the complex and for the receptor, showing that the host-guest exchange is fast on the NMR time scale. As the aromatic protons of the CTV unit display sharp well-defined signals without overlap with other ones, their complexation-induced shifts were plotted as a function of the guest/host ratio (Figures S22-S27). In light of recent articles dealing with the stoichiometry of host/guest complexes and the determination of the related binding constants, titration curves were fitted with different models, i.e. stoichiometry,

using Bindfit program, instead of performing Job's plot experiments.[18,19] In all cases the better fit was obtained with a 1:1 host:guest stoichiometry, which is in agreement with the mass analysis of the (-)-**3** and Oct-β-Glc mixture (Figure S20). From the resulting association constants reported in Table 1 several features can be underlined. (i) Firstly, good association constants up to 10^3 M^{-1} can be reached, in particular for the binding of Oct-β-Glc by (-)-**3**. (ii) Secondly, the enantioselectivity remains high: an enantioselectivity of 96:4 is reached between (-)-**3** and (+)-**3** for the recognition of Oct-β-Glc, with binding constants of 993 and 45 M^{-1} respectively. It is all the more remarkable that the enantioselectivity of the recognition process is only controlled by the inherent chirality of the CTV moiety. This is in sharp contrast with most of the previous hemicryptophane cages used to complex enantioselectively carbohydrates, which involved additional stereogenic units (center or axis).[17] This enantioselectivity is even exclusive with galactose derivatives since no recognition occurs with the receptor (+)-**3** whereas host (-)-**3** displays binding constants of 245 M^{-1} and 274 M^{-1} for Oct-α-Gal and Oct-β-Gal guest, respectively. (iii) Good α/β discrimination can be also achieved with these receptors: the binding constant is ten times higher for Oct-β-Glc than for Oct-α-Glc with (-)-**3** as receptor (993 M^{-1} and 100 M^{-1}, respectively), and 30 times higher for Oct-α-Man than for Oct-β-Man with (-)-**3** as receptor (218 M^{-1} and 7 M^{-1}, respectively). (iv) Whereas the (-)-**3** enantiomer is Oct-β-Glc-selective with a selectivity from moderate to high (a selectivity of 3.6:1 and 141:1 when compared to Oct-β-Gal and Oct-β-Man, respectively), the (+)-**3** enantiomer displays an Oct-Man selectivity, with a binding constant up to 856 M^{-1}, for Oct-β-Man and less than 45 M^{-1} for other glucose and galactose derivatives. This change in substrate selectivity suggests different orientations and interactions of Oct-β-Glc and Oct-Man inside the cavities of (-)-**3** and (+)-**3** respectively. As the abilities of carbohydrates to induce intermolecular hydrogen bonds is the following: Oct-α-Man > Oct-β-Man > Oct-β-Glc > Oct-α-Glc > Oct-α-Gal ≥ Oct-β-Gal,[20,21] hydrogen bonds play probably a more important role in the formation of Oct-α-Man@(+)-**3** than in the in the case of the Oct-β-Glc@(-)-**3**.

.

Table 1. Binding constants K_a (M^{-1}) for the 1:1 complexes formed between the different isomers of host **3** and the carbohydrate guests.[a]

Guest	Host	K_a ($L.mol^{-1}$)	Enantioselectivity
Oct-β-Glc	(-)-**3**	993 ± 7.3%	96:4
	(+)-**3**	45 ± 3.1%	
Oct-β-Gal	(-)-**3**	274 ± 3.2%	> 99.5:0.5
	(+)-**3**	-[b]	
Oct-β-Man	(-)-**3**	7 ± 2.3%	1:99
	(+)-**3**	856 ± 7.8%	
Oct-α-Glc	(-)-**3**	100 ± 3.2%	77:23
	(+)-**3**	30 ± 1.4%	
Oct-α-Gal	(-)-**3**	245 ± 4.7%	> 99.5:0.5
	(+)-**3**	-[b]	
Oct-α-Man	(-)-**3**	218 ± 2.1%	30:70
	(+)-**3**	508 ± 5.2%	

[a] K_a was determined by fitting ^{1}H NMR titration curves ($CDCl_3$, 500 MHz, 298 K) on the aromatic protons of the CTV unit (δ at 6.90 ppm for the free host) with Bindfit program. More details on the calculations results (covariance and RMS) can be found in Table S4; estimated error 10%. [b] No complexation detected.

Conclusions

In summary, we have described the synthesis of a new chiral hemicryptophane cage. Its resolution has allowed investigating the stereoselective recognition properties of the two enantiomers toward six carbohydrate stereoisomers. In sharp contrast with other hemicryptophane derivatives, this new host combines both good binding constants (up to 10^3 M^{-1}) and remarkable enantioselectivity (exclusive in some cases). Moreover, depending on the enantiomer of the receptor used, a strong change in substrate

selectivity is observed, allowing to choose the most appropriate hemicryptophane enantiomer to complex selectively the desired sugar derivative.

Experimental Section

Chemicals and materials.

Starting material and solvents were of commercial grade and were used without further purification. Chromatography was carried out with Merck 60 A (0.040 - 0.063 mm) silica gel. TLC was performed with Merck silica gel 60 F254 plates. Melting points were determined with a Büchi Melting Point B-545. IR spectra were obtained using a Bruker Alpha Platinium ATR. ^{1}H NMR and ^{13}C NMR were recorded at 298 K on a Bruker Avance III HD 300 MHz spectrometer and a Bruker Avance III HD 400 MHz. ^{1}H NMR and ^{13}C NMR chemical shifts δ are reported in ppm referenced to the protonated residual solvent signal. HRMS were performed on a SYNAPT G2 HDMS (Waters) mass spectrometer with API and spectra were obtained with TOF analysis. Measurements were realized with two internal standards. ECD spectra were recorded on a Jasco J-815 spectrometer in CH_2Cl_2.

CTV-derivative 4.

Compound **4** was prepared according to the published procedure.[13]

Synthesis of 5.[22]

In a dry 100 mL round-bottom flask, compound **4** (1.30 g, 1.78 mmol) was dissolved in dry DMF (40 mL) and sodium azide (1.16 g, 17.8 mmol) was added portion-wise. The mixture was stirred at 60 °C overnight. Solvent was partially removed under reduced pressure and the resulting crude mixture was diluted with CH_2Cl_2 (50 mL). Water was added (50 mL) and the layers were separated. The aqueous layer was extracted with CH_2Cl_2 (30 mL). The organic layers were combined, washed with water (3 x 30 mL), dried over $MgSO_4$. A yellowish oil was obtained after evaporation of the solvent under reduced pressure. Diethyl ether (70 mL) was added and the mixture was stored at 4°C for about 6 hours to give a white solid which was filtered on a frit and washed with Et_2O to yield **5** (990 mg, 90 %). ^{1}H NMR ($CDCl_3$, 300 MHz, 298 K) δ 6.93 (s, 3H), 6.85 (s, 3H), 4.75 (d, J = 13.7 Hz, 3H), 4.14 (t, J = 5.2 Hz, 6H), 3.83 (s, 9H), 3.59–3.52 (m, 9H); ^{13}C NMR ($CDCl_3$, 75 MHz, 298 K) δ

149.2, 146.5, 133.9, 131.9, 118.1, 114.2, 69.2, 56.2, 50.3, 36.4; IR σ = 2931, 2110, 1511, 1265 cm^{-1}; HRMS (ESI-TOF) m/z: $[M + Na]^+$ Calcd for $C_{30}H_{33}N_9O_6Na$ 638.2446; Found 638.2442; R_f = 0.23 (CH_2Cl_2); m.p. = 137–138 °C.

Synthesis of 6.

Compound **5** (490 mg, 0.796 mmol) was dissolved in THF (15 mL) and water (0.5 mL) and triphenylphosphine (3.75 g, 14.3 mmol) was slowly added at 0 °C. The reaction mixture was stirred at r.t. for 16 h and solvent was removed under reduced pressure. Diethyl ether (50 mL) was added to the resulting solid and the mixture was stirred at r.t. for 24 h. Filtration afforded compound **6** as a white powder (391 mg, 91 %). ^{1}H NMR ($CDCl_3$, 400 MHz, 298 K) δ 6.88 (s, 3H), 6.82 (s, 3H), 4.75 (d, J = 13.7 Hz, 3H), 4.07–3.92 (m, 6H), 3.82 (s, 9H), 3.53 (d, J = 13.4 Hz, 3H), 3.05 (t, J = 5.2 Hz, 6H); ^{13}C NMR ($CDCl_3$, 100 MHz, 298 K) δ 148.5, 147.1, 132.6, 131.9, 116.1, 113.8, 72.0, 56.2, 41.6, 36.5; IR σ = 3430, 2935, 1511, 1263 cm^{-1}; HRMS (ESI-TOF) m/z: $[M + H]^+$ Calcd for $C_{30}H_{40}N_3O_6$ 538.2912; Found 538.2913; R_f= 0.05 (CH_2Cl_2/MeOH : 97/3); m.p. = 174–176 °C.

Synthesis of 7.[23]

To a solution of salicylaldehyde (158 µL, 1.52 mmol) in absolute ethanol (20 mL) was added NaOH (66 mg, 1.65 mmol). The reaction mixture was stirred at r.t. for 40 minutes and a solution of 1,3,5-tris(bromomethyl)benzene (151 mg, 0.423 mmol) in absolute ethanol (7 mL) was added. The mixture was refluxed for 20 h and cooled to 4 °C overnight. The resulting solid was filtered off and washed with cold ethanol and cold water to afford trialdehyde **7** as a white powder (165 mg, 78 %). ^{1}H NMR ($CDCl_3$, 300 MHz, 298 K) δ 10.53 (s, 3H), 7.87 (dd, J = 7.7; 1.7 Hz, 3H), 7.58–7.52 (m, 6H), 7.07 (dd, J = 17.2; 8.1 Hz, 6H), 5.25 (s, 6H); ^{13}C NMR ($CDCl_3$, 75 MHz, 298 K) 189.7, 160.9, 137.7, 136.2, 129.0, 126.0, 125.4, 121.5, 113.2, 70.2; IR σ = 3053, 2842, 1677, 1604, 1392, 1269 cm^{-1}; HRMS (ESI-TOF) m/z: $[M + NH_4]^+$ Calcd for $C_{30}H_{28}NO_6$ 498.1911; Found 498.1915; R_f= 0.32 (CH_2Cl_2); m.p. = 135–137 °C.

Synthesis of hemicryptophane 3.

To a solution of compound **6** (179 mg, 0.333 mmol) in a 1/1 mixture of $CHCl_3$/MeOH (120 mL) was added dropwise a solution of trialdehyde **7** (147 mg, 0.306 mmol) in the same mixture of solvents

(80 mL). The reaction mixture was stirred overnight at r.t. and $NaBH_4$ (407 mg, 10.7 mmol) was added portionwise at 0 °C. The mixture was stirred at r.t. for 4 h and solvents were removed under reduced pressure. The crude residue was dissolved in $CHCl_3$ (60 mL) and washed with a 10 % NaOH solution (30 mL). Aqueous phase was extracted with $CHCl_3$ (2 x 20 mL) and combined organic layers were washed with a 10 % NaOH solution (40 mL), dried over $MgSO_4$. The organic solvent was removed under reduced pressure to afford a white solid which was purified by column chromatography ($CHCl_3$/MeOH/Et_3N, gradient from 97/1/2 to 90/8/2). Racemic hemicryptophane **3** was obtained as a white solid (126 mg, 42 %).

The resolution of the racemic mixture was performed by chiral HPLC using a Chiralpak ID (250 x 10 mm) column with EtOH + Et_3N / CH_2Cl_2 (50/50) as mobile phase (see supporting information) to yield the two enantiopure hemicryptohane (-)-**3** (30 mg, ee > 99.5%) and **(+)-3** (34 mg, ee > 98.5%).

^{1}H NMR ($CDCl_3$, 400 MHz, 298 K) δ 7.21 (dd, J = 7.3; 1.6 Hz, 3H), 7.08 (td, J = 8.0; 1.6 Hz, 3H), 6.97 (s, 3H), 6.87 (t, J = 7.1 Hz, 6H), 6.78 (s, 3H), 6.58 (d, J = 8.0 Hz, 3H), 4.73 (d, J = 13.7 Hz, 3H), 4.28–4.14 (m, 12H), 3.95 (d, J = 13.2 Hz, 3H), 3.88–3.81 (m, 3H), 3.62 (s, 9H), 3.53 (d, J = 13.8 Hz, 3H), 3.49 (br s, 3H), 3.13–3.05 (m, 3H), 2.99–2.92 (m, 3H); ^{13}C NMR ($CDCl_3$, 100 MHz, 298 K) δ 156.3, 149.0, 146.5, 137.1, 132.0, 131.0, 130.9, 129.5, 126.9, 121.0, 113.6, 112.1, 69.1, 68.6, 56.1, 48.8, 47.3, 36.4; IR σ = 3438, 2929, 1602, 1510, 1490, 1457, 1263, 1220 cm^{-1}; HRMS (ESI-TOF) m/z: $[M + H]^+$ Calcd for $C_{60}H_{64}N_3O_9$ 970.4637; Found 970.4639; R_f= 0.06 ($CHCl_3$/MeOH/Et_3N: 96/2/2); m.p. = 299–302 °C;

M (-): $[\alpha]_D^{25}$ = - 79 (*c* 0.15, CH_2Cl_2).

P (+): $[\alpha]_D^{25}$ = + 78 (*c* 0.235, CH_2Cl_2).

^{1}H NMR titrations.

A solution of enantiopure host **3** (1.0 mM in $CDCl_3$, 500 µL) was titrated in NMR tubes with aliquots of a concentrated solution (10 mM in the same solvent) of carbohydrates. The shifts $\Delta\delta$ of the host's protons signals at 6.90 ppm were measured after each addition and plotted as a function of the guest/host ratio ([G]/[H]). Association constant K_a was obtained by nonlinear least-squares fitting of

these plots using Bindfit program from Thordarson's group[19]. K_a, covariance and RMS are reported for each carbohydrate in the supporting information.

AUTHOR INFORMATION

Corresponding Author

E-mail: alexandre.martinez@centrale-marseille.fr

Notes The authors declare no competing financial interest.

ASSOCIATED CONTENTS

Supporting Information

^{1}H, ^{13}C NMR spectra, CD and mass spectra of compounds **5, 6, 7, 3**; HPLC analysis; titration experiments; calculation methods.

REFERENCES

(1) Wong, C.-H. Carbohydrate-Based Drug Discovery, Wiley-VCH, Weinheim, 2003.

(2) Roth, J. *Chem. Rev.* **2002**, *102*, 285–304.

(3) Angata, T.; Varki, A. *Chem. Rev.* **2002**, *102,* 439–470.

(4) Ernst, B.; Hart, G. W.; Sinaý, P. Carbohydrates in Chemistry and Biology, Wiley-VCH, Weinheim, 2000.

(5) Tohda, K.; Gratzl, M. *ChemPhysChem* **2003**, *4*, 155–161.

(6) For reviews see: a) Mazik, M. *Chem. Soc. Rev.* **2009**, *38*, 935–956; b) Davis, A. P. *Org. Biomol. Chem.* **2009**, *7*, 3629–3638.

(7) For more recent exemples: a) Francesconi, O.; Gentili, M.; Nativi, C.; Ardá, A.; Cañada, F. J.; Jiménez-Barbero, J.; Roelens, S. *Chem. Eur. J.* **2014**, *20*, 6081–6091; b) Chandramouli, N.; Ferrand, Y.; Lautrette, G.; Kauffmann, B.; Mackereth, C. D.; Laguerre, M.; Dubreuil, D.; Huc, I. *Nat. Chem.* **2015**, *7*, 334–341; c) Mooibroek, T. J.; Casas-Solvas, J. M.; Harniman, R. L.; Renney, C. M.; Carter, T. S.; Crump, M. P.; Davis, A. P. *Nat. Chem*. **2015**, *8*, 69–74; d) Mooibroek, T. J.; Crump, M. P.; Davis, A. P. *Org. Biomol. Chem*. **2016**, *14*, 1930–1933; e) Lippe, J.; Seichter, W.; Mazik, M. *Org.*

Biomol. Chem. **2015**, *13*, 11622–11632; f) Amrhein, F.; Lippe, J.; Mazik, M. *Org. Biomol. Chem.* **2016**, *14*, 10648–10659; g) Ríos, P.; Mooibroek, T. J.; Carter, T. S.; Williams, C.; Wilson, M. R.; Crump, M. P.; Davis, A. P. *Chem. Sci*. **2017**, *8*, 4056–4061; h) Mandal, P. K.; Kauffmann, B.; Destecroix, H.; Ferrand, Y.; Davis, A. P.; Huc, I. *Chem. Commun*. **2016**, *52*, 9355–9358; i) Gunasekara, R. W.; Zhao, Y. *J. Am. Chem. Soc*. **2017**, *139*, 829–835; j) Yabushita, M.; Li, P.; Bernales, V.; Kobayashi, H.; Fukuoka, A.; Gagliardi, L.; Farha, O. K.; Katz, A. *Chem. Commun*. **2016**, *52*, 7094–7097; k) Hwang, J. Y.; Jeon, H.-G.; Choi, Y. R.; Kim, J.; Kang, P.; Lee, S.; Jeong, K.-S. *Org. Lett*. **2017**, *19*, 5625–5628.

(8) a) Hardie, M. J. *Chem. Soc. Rev*. **2010**, *39*, 516–527; b) Lefevre, S.; Heloin, A.; Pitrat, D.; Mulatier, J.-C.; Vanthuyne, N.; Jean, M.; Dutasta, J.-P.; Guy, L.; Martinez, A. *J. Org. Chem*. **2016**, *81*, 3199–3205.

(9) Lefevre, S.; Simonet, R.; Pitrat, D.; Mulatier, J.-C.; Vanthuyne, N.; Jean, M.; Dutasta, J.-P.; Guy, L.; Martinez, A. *ChemistrySelect* **2016**, *1*, 6316–6320.

(10) Zhang, D.; Martinez, A.; Dutasta, J.-P. *Chem. Rev.* **2017**, *117*, 4900–4942.

(11) Schmitt, A.; Chatelet, B.; Padula, D.; Bari, L. D.; Dutasta, J.-P.; Martinez, A. *New J. Chem.* **2015**, *39*, 1749–1753.

(12) Perraud, O.; Martinez, A.; Dutasta, J.-P. *Chem. Commun*. **2011**, *47*, 5861–5863.

(13) Chatelet, B.; Payet, E.; Perraud, O.; Dimitrov-Raytchev, P.; Chapellet, L.-L.; Dufaud, V.; Martinez, A.; Dutasta, J.-P. *Org. Lett*. **2011**, *13*, 3706–3709.

(14) a) Canceill, J.; Collet, A.; Gabard, J.; Gottarelli, G.; Spada, G. P. *J. Am. Chem. Soc*. **1985**, *107*, 1299–1308; b) Canceill, J.; Collet, A.; Gottarelli, G.; Palmieri, P. *J. Am. Chem. Soc.* **1987**, *109*, 6454–6464.

(15) Ardá, A.; Venturi, C.; Nativi, C.; Francesconi, O.; Cañada, F. J.; Jiménez-Barbero, J.; Roelens, S. *Eur. J. Org. Chem.* **2010**, *75*, 64–71.

(16) Francesconi, O.; Gentili, M.; Roelens, S. *J. Org. Chem*. **2012**, *77*, 7548–7554.

(17) Zhang, D.; Mulatier, J.-C.; Cochrane, J. R.; Guy, L.; Gao, G.; Dutasta, J.-P.; Martinez, A. *Chem. Eur. J.* **2016**, *22*, 8038–8042.

(18) Ulatowski, F.; Dąbrowa, K.; Bałakier, T.; Jurczak, J. *J. Org. Chem*. **2016**, *81*, 1746–1756.

(19) Hibbert, D. B.; Thordarson, P. *Chem. Commun*. **2016**, *52*, 12792–12805; URL: http://app.supramolecular.org/bindfit/

(20) Bonar-Law, R. P.; Sanders, J. K. M. *J. Am. Chem. Soc*. **1995**, *117*, 259–271.

(21) López de la Paz, M.; Ellis, G.; Pérez, M.; Perkins, J.; Jiménez-Barbero, J.; Vicent, C. *Eur. J. Org. Chem.* **2002**, 840–855.

(22) Wang, L.; Wang, G.-T.; Zhao, X.; Jiang, X.-K.; Li, Z.-T. *J. Org. Chem*. **2011**, *76*, 3531–3535.

(23) Le Gac, S.; Zeng, X.; Girardot, C.; Jabin, I. *J. Org. Chem*. **2006**, *71*, 9233–9236.